ACS APPLIED MATERIALS & INTERFACES

RESEARCH ARTICLE

www.acsami.org

Double-Electrochromic Coordination Polymer Network Films

Anna Maier, Kalie Cheng, Julia Savych, and Bernd Tieke*

Department für Chemie, Universität zu Köln Luxemburger Str. 116, D-50939 Köln, Germany

Supporting Information

ABSTRACT: Formation and characteristic properties of organized double-electrochromic films consisting of electrochromic poly(4-(2,2′:6,2″-terpyridyl)phenyliminofluorene) (**P-1**)-zinc ion complexes and electrochromic anions are reported. The anions are 2,2′-azino-bis(3-ethylbenzo-thiazoline-6-sulfonate) (**ABTS**) and poly((4-sulfonatophenyl)iminofluorene) (**P-2**). The films were prepared upon multiple sequential adsorption of **P-1** and the zinc salts of **ABTS** and **P-2** on solid supports using coordinative interactions between the Zn ions and the terpyridine (tpy) ligands. The **ABTS** and **P-2** ions are incorporated in the films via electrostatic forces neutralizing the charge of the complexed divalent zinc (Zn^{2+}) ions. The optical, electrochemical, and electrochromic properties of the films are described. Films consisting of the Zn ion complex of **P-1** and **ABTS** are yellow in the neutral state and change their color to brownish gray and finally blue, if anodically oxidized at ~640 mV vs FOC. Films containing the Zn ion complex of **P-1**, with **P-2** as a counterion, are yellow in the neutral state and change color to dark red and finally blue, if anodically oxidized at ~450 mV vs FOC. Compared with previously reported films of the Zn ion complex of **P-1** with nonelectroactive hexafluorophosphate as the counterion, the new films exhibit faster response times, as well as higher contrast, and the colors in the oxidized state are modified. The films are stable under ambient conditions and might be useful as active layers in electrochromic devices.

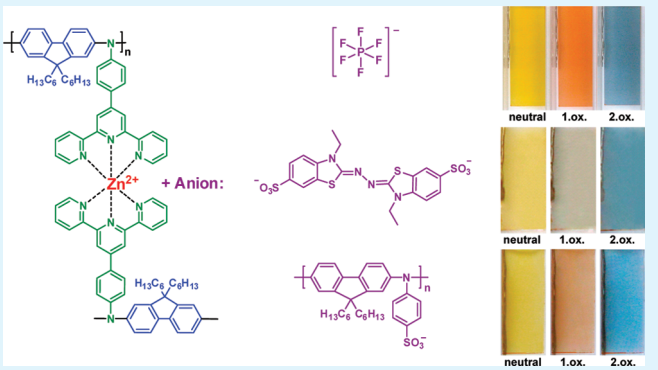

KEYWORDS: electrochromism, coordination polymer, self-assembly, zinc-terpyridine complex, ABTS, polyiminofluorene, polyelectrolyte

1. INTRODUCTION

Electrochromic materials are known to undergo reversible color changes in response to externally applied potentials.[1−4] Current interest in these materials originates from their spectral and electrochemical properties, and their application potential in electrochromic displays, smart windows, chameleon materials, and variable reflectance mirrors.[5] Inorganic materials[6] (such as transition-metal oxides and Prussian Blue (PB)-type materials) and organic materials[7−9] (such as conjugated polymers, viologens, and triarylamine derivatives) are suitable for this purpose. Conjugated polymers are especially useful, because of their easy processing into uniform, transparent, and amorphous films using solution-casting, spin-coating, or electropolymerization. Besides the conventional processing methods, layer-by-layer (LbL) assembly techniques[10−12] represent a useful alternative, especially when films with thickness control in the nanometer range are in demand. LbL assembly on solid supports is either based on electrostatic interactions,[10] hydrogen bonding,[11] or coordinative interactions[12] between suitable building blocks, which are sequentially adsorbed on the substrate from solution. Previous examples of electrochromic LbL assemblies were mainly based on conjugated polymers such as polyaniline,[13] polythiophene,[8b,14] polymers containing viologen[8b,15] or triphenylamine units,[16] or colloidal particles of PB derivatives,[13,17] which were adsorbed by means of electrostatic interactions. The disadvantage of these films is that usually nonelectroactive polyelectrolytes must be coadsorbed as counterions, which subsequently "dilute" the electrochromic behavior by reducing the contrast and increasing the response times.

A new type of electrochromic film, showing high contrast and fast switching times, was reported only recently.[18−20] The films were prepared upon coordinative assembly of metal salts and conjugated polymers containing terpyridine (tpy) ligands as substituent groups. The tpy ligands enable the coordination of divalent and trivalent metal ions and the formation of bis-tpy complexes with D_{2d} symmetry.[21] While complex formation of ditopic ligands and metal ions leads to linear coordination polymer chains,[22] the complex formation of the polytopic ligands with metal ions leads to coordination polymer network structures.[18−20,23] Recent studies were concerned with films consisting of tpy-functionalized polyiminofluorene (**P-1**) (Scheme 1),[18,19] or tpy-functionalized polyiminocarbazole,[20] and zinc, cobalt, or nickel hexafluorophosphate as metal salt. The studies have shown that the electrochromic behavior of the films can be widely modified, e.g., by variation of the

Received: April 21, 2011
Accepted: June 16, 2011
Published: June 16, 2011

Scheme 1. Syntheses of P-1 and P-2

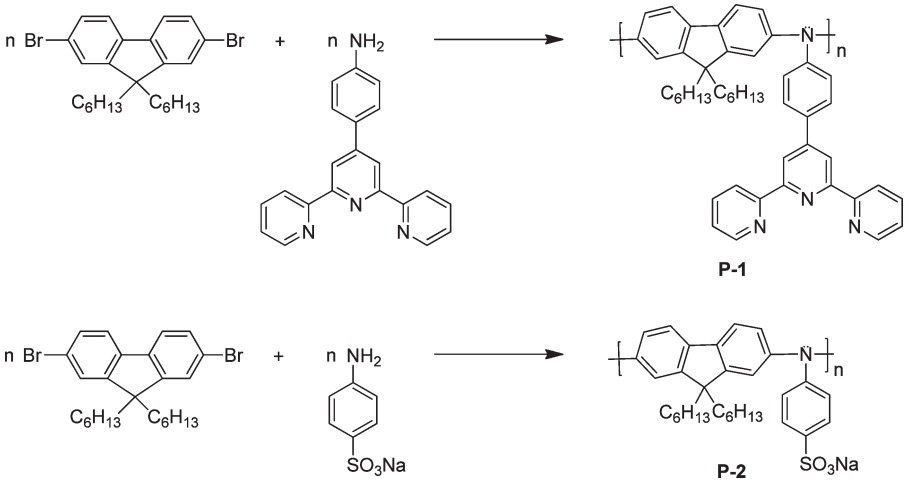

Scheme 2. Neutral and Oxidized States of ABTS Dianion

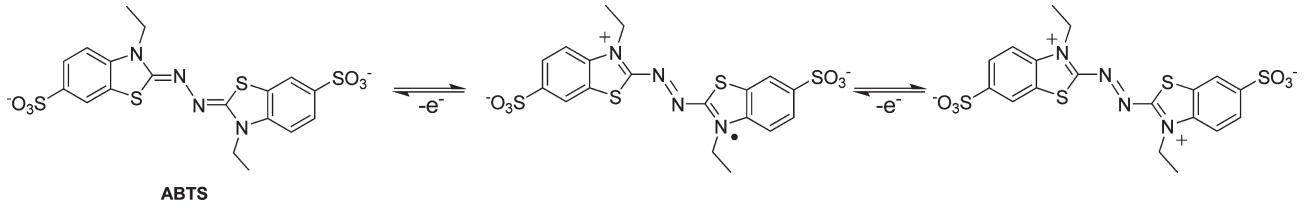

Scheme 3. Neutral and Oxidized States of P-2 Polyanion

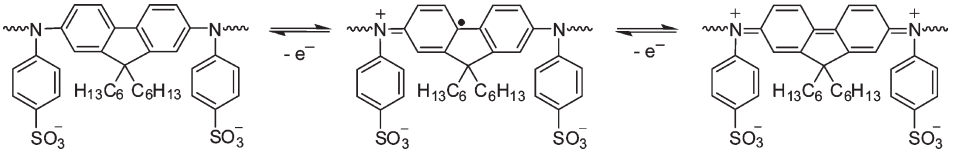

metal ions[19] or the aromatic unit of the polyiminoarylene backbone of the polytopic ligand.[20] In a continuation of this work, we now demonstrate that the electrochromic behavior can be altered and improved using metal salts with organic electroactive counterions instead of hexafluorophosphate salts. The counterions neutralize the positive charge of the metal ions complexed by the tpy groups and are therefore incorporated in the films. In contrast to previous work, we now use dipping solutions containing zinc salts with organic electrochromic dianions and polyanions, instead of nonelectroactive zinc hexafluorophosphate and built-up double-electrochromic films containing the electrochromic polyiminofluorene-tpy Zn ion complex and electrochromic anions.

The purpose of the present paper is to describe the effects of the organic electroactive anions on the spectral and electrochemical behavior of the films, and on their electrochromic properties, such as the color in the neutral and oxidized state, contrast, and switching time. As electrochromic anions, 2,2′-azino-bis(3-ethyl-benzothiazoline-6-sulfonate) (**ABTS**)[24−26] and poly((4-sulfonatophenyl)iminofluorene) (**P-2**) were used (see Scheme 1). **ABTS** can be easily oxidized under formation of the cation radical and dication state (see Scheme 2). **P-2** contains the same polyiminofluorene main chain as **P-1**. Similarly, it can be easily oxidized under formation of the cation radical and dication state (see Scheme 3). In our study, we report on film preparation and characteristic properties of the resulting films using UV/vis spectroscopy and cyclic voltammetry. It is demonstrated that the incorporation of the organic conjugated anions alters the electrochromic properties of the films by changing the colors, shortening the response time, and improving the contrast.

2. EXPERIMENTAL SECTION

Materials. Polyallylamine hydrochloride (PAH, molecular weight (mw) of 15.000 g/mol) and sodium polystyrene sulfonate (PSS, mw = 70.000 g/mol) were purchased from Aldrich. Polyethyleneimine (PEI, branched, mw = 70.000 g/mol, 30% aqueous solution) was purchased from Polyscience, Inc., and used without further purification. Sodium 4-aminobenzenesulfonate was obtained from Fluka. **P-1** was prepared as previously described.[27] Dipalladium tri(dibenzylideneacetone), tris-*t*-butylphosphine, and sodium *t*-butoxide were obtained from Acros and Fluka and used without further purification. Zinc acetate, $Zn(OAc)_2 \cdot 2H_2O$, was obtained from Merck. Potassium hexafluorophosphate and 2,2′-azino-bis(3-ethylbenzothiazoline-6-sulfonic acid)

(**ABTS**) diammonium salt were purchased from Aldrich. Both salts were used without further purification. Tetrahydrofuran (THF) was distilled over sodium hydride under nitrogen. *N*,*N*-Dimethylformamide (DMF) was distilled over calcium hydride. Acetonitrile (HPLC grade), methanol (MeOH), *n*-hexane, and tetrabutylammonium hexafluorophosphate ($TBAPF_6$) were obtained from Acros and Aldrich and used without further purification.

Synthesis of P-2. Sodium 4-aminobenzenesulfonate (0.070 g (0.406 mmol)) and 2,7-dibromo-9,9-dihexylfluorene (0.20 g (0.406 mmol))[28] were dissolved in 10 mL of *t*-butanol under inert conditions, using the Schlenk tube technique. To this solution were added 0.0093 g (10.1 μmol) of $Pd_2(dba)_3$, 0.0124 g (61.4 μmol) of tris-*t*-butylphosphine, and, finally, 0.195 g (2.03 mmol) of sodium *t*-butoxide. The reaction mixture was stirred under nitrogen at 100 °C for 24 h. After cooling to room temperature, dichloromethane (DCM) was added in order to precipitate the polymer. The product was filtered and washed several times with DCM/acetone (1:1). A small portion (0.180 g) of a beige powder was obtained. Yield: 88%. Matrix-assisted laser desorption ionization−time of flight (MALDI-TOF) measurements indicate the trimer and tetramer to be the most frequent species.

^{1}H NMR (300 MHz, DMSO-d_6, ppm): δ 7.86 (d, 1H, arom. fluorene); 7,80 (d, 1H, arom. fluorene); 7.61 (s, 1H, arom. fluorene); 7.48 (d, 1H, arom. fluorene); 7.25 (d, 2H, phenyl-H); 7.11 (s, 1H, arom. fluorene); 6.92 (d, 1H, arom. fluorene); 6.44 (d, 2H, phenyl-H); 0.73−1.75 (m, 26H; alkyl chain). UV (Abs., λ_{max}, DMSO): 368 nm; (Fluorescence, λ_{max}, DMSO): 422 nm. Fluorescence quantum yield (DMSO, λ_{exc} = 365 nm): 0.45.

Substrates. Quartz substrates (30 mm × 12 mm × 1 mm) were cleaned in a fresh piranha solution (7:3 mixture of 98% H_2SO_4/30% H_2O_2. [***Caution:*** *The mixture is strongly oxidizing and may detonate upon contact with organic material.*] The solution mixture was then washed with Milli-Q water and was successively subjected to ultrasonication in alkaline isopropanol, and 0.1 M aqueous HCl, at 60 °C for 1 h each. After careful washing with Milli-Q water, the substrates were silanized with 3-aminopropylmethyldiethoxysilane (Fluka) in toluene, and finally coated with three polyelectrolyte layers in the sequence PSS−PEI−PSS, as previously described.[29] The precoating provides a highly charged surface onto which the metal ions can be adsorbed in high concentration.

Indium tin oxide (ITO)-coated glass substrates were cleaned upon ultrasonication in ethanol and water at 60 °C for 30 min each. Two polyelectrolyte layers then were deposited, in the sequence PEI−PSS, in the same way as that reported for the quartz substrates.

METHODS

Film Preparation. *P-1/Zn-ABTS* *Films.* The dipping solution of zinc 2,2′-azino-bis(3-ethylbenzothiazoline-6-sulfonate) (**Zn-ABTS**) was prepared by mixing equal volumes of a 0.01 M solution of **ABTS** diammonium salt in MeOH/THF/*n*-hexane (2:1:1 v/v) and a 0.01 M solution of zinc acetate in the same solvent mixture. The pretreated substrates were dipped into (a) the solution of **Zn-ABTS**, (b) MeOH/THF/*n*-hexane (2:1:1 v/v), (c) MeOH/THF/*n*-hexane (2:1:1 v/v), (d) a 5 × 10^{-4} monomolar solution of **P-1** in THF/*n*-hexane (2:1 v/v), (e) THF/*n*-hexane (2:1 v/v), (f) THF/*n*-hexane (2:1 v/v), and, again, the sequence (a)−(f) was applied, etc. Immersion times were 5 min each for steps (a) and (d), and 30 s for steps (b), (c), (e), and (f).

P-1/Zn-P-2 *Films.* The dipping solution of **Zn-P-2** was prepared by mixing equal volumes of a 0.004 monomolar solution of **P-2** in MeOH with a 0.002 M solution of zinc acetate in MeOH. The pretreated substrates were dipped into (a) the solution of **Zn-P-2**, (b) MeOH, (c) MeOH, (d) a 5 × 10^{-4} monomolar solution of **P-1** in THF/*n*-hexane (1:1 v/v), (e) THF/*n*-hexane (1:1 v/v), (f) THF/*n*-hexane), and, again, the sequence (a)−(f) was applied, etc. Immersion times were 10 min each for steps (a) and (d), and 30 s for steps (b), (c), (e), and (f).

^{1}H NMR spectra were recorded on a Bruker Model AC 300 spectrometer operating at 300 MHz. UV−visible absorption spectra were recorded using a Perkin−Elmer Model Lambda 14 spectrometer. All spectra were corrected by subtracting the signal of the precoated quartz substrate. Electrochemical experiments were performed on a Heka potentiostat/galvanostat (Model PG 390, Heka Electronic, Lambrecht, Germany). Data acquisition and potentiostat control were accomplished using the Potpulse software, version 8.4 (Heka). All experiments were carried out in a conventional three-electrode glass electrochemical cell at room temperature, employing the polymer film on an ITO-coated glass substrate; reference and counter electrodes were platinum. The experiments were carried out in acetonitrile (saturated with N_2) containing 0.1 M tetrabutylammonium hexafluorophosphate ($TBAPF_6$) as electrolyte salt. Film thickness was measured with a Model Dektak 3 apparatus from Vecco. The film was partially scratched from the surface, and a height profile of the surface was scanned. The error in the measurements was ±2.5 nm.

3. RESULTS AND DISCUSSION

3.1. Preparation of the Polymers. The preparation of the polytopic ligand poly(4-(2,2′:6,2″-terpyridyl)phenyliminofluorene) (**P-1**) with terpyridyl-phenyl units attached to the N atoms of the polymer chain and the new anionic compound poly ((4-sulfonatophenyl)iminofluorene) (**P-2**) follows a general procedure recently described for polyiminoarylenes by Kanbara et al.[30] outlined in Scheme 1. The polycondensation of 2,7-dibromo-9,9-dihexyl-fluorene[28] and 4′-(*p*-aminophenyl)-2,2′:6,2″-terpyridine[27] was carried out under inert conditions in a toluene/dioxane solvent mixture (3:2, v/v) at 100 °C, the reaction time was 10 h. The $Pd_2(dba)_3$/ X-Phos system was used as a catalyst, and sodium *t* -butoxide was used as a base. Details of the synthesis were recently described.[27] A MALDI-TOF study of the molecular weight distribution showed oligomers up to the hexadecamer, with the pentamer to the octamer being the most frequent species.

P-2 was prepared upon reaction of 2,7-dibromo-9,9-dihexyl-fluorene with sodium 4-aminobenzenesulfonate. In this reaction, $Pd_2(dba)_3$/tris-*t*-butyl-phosphine was used as the catalyst, and sodium *t*-butoxide was used as the base again (see Scheme 1). The detailed protocol is given in the Experimental Part. The ^{1}H NMR spectrum is shown in the Supporting Information. The spectrum displays all the expected resonances of the alkyl chain protons at 0.73−1.75 ppm, the protons of the *N*-phenyl group at 6.44 and 7.25 ppm, and the aromatic protons of the fluorene rings at 6.92, 7.11, 7.48, 7.61, 7.80, and 7.86 ppm. **P-2** was obtained as beige powder that was soluble in polar organic solvents such as dimethylsulfoxide, methanol, acetone, and water. Solutions exhibit a pale yellow color and a blue fluorescence, with a maximum at 422 nm and a quantum yield of 45% in dimethyl sulfoxide (DMSO). A MALDI-TOF study of the molecular weight distribution showed maximum peaks corresponding to the trimer and tetramer. This indicates the formation of an oligomeric anion. The redox-active dianionic compound 2,2′-azino-bis (3-ethylbenzothiazoline-6-sulfonate) (**ABTS**) was commercially available as the diammonium salt. It was converted into the zinc salt as described in the Experimental Part.

3.2. Complex Formation of P-1 with Zn-ABTS in Solution. Before we studied the layer-by-layer assembly of the terpyridine-containing polytopic ligand **P-1** and **Zn-ABTS**, we investigated

Scheme 4. Complex Formation of P-1 with (a) Zn-ABTS and (b) Zn-P-2

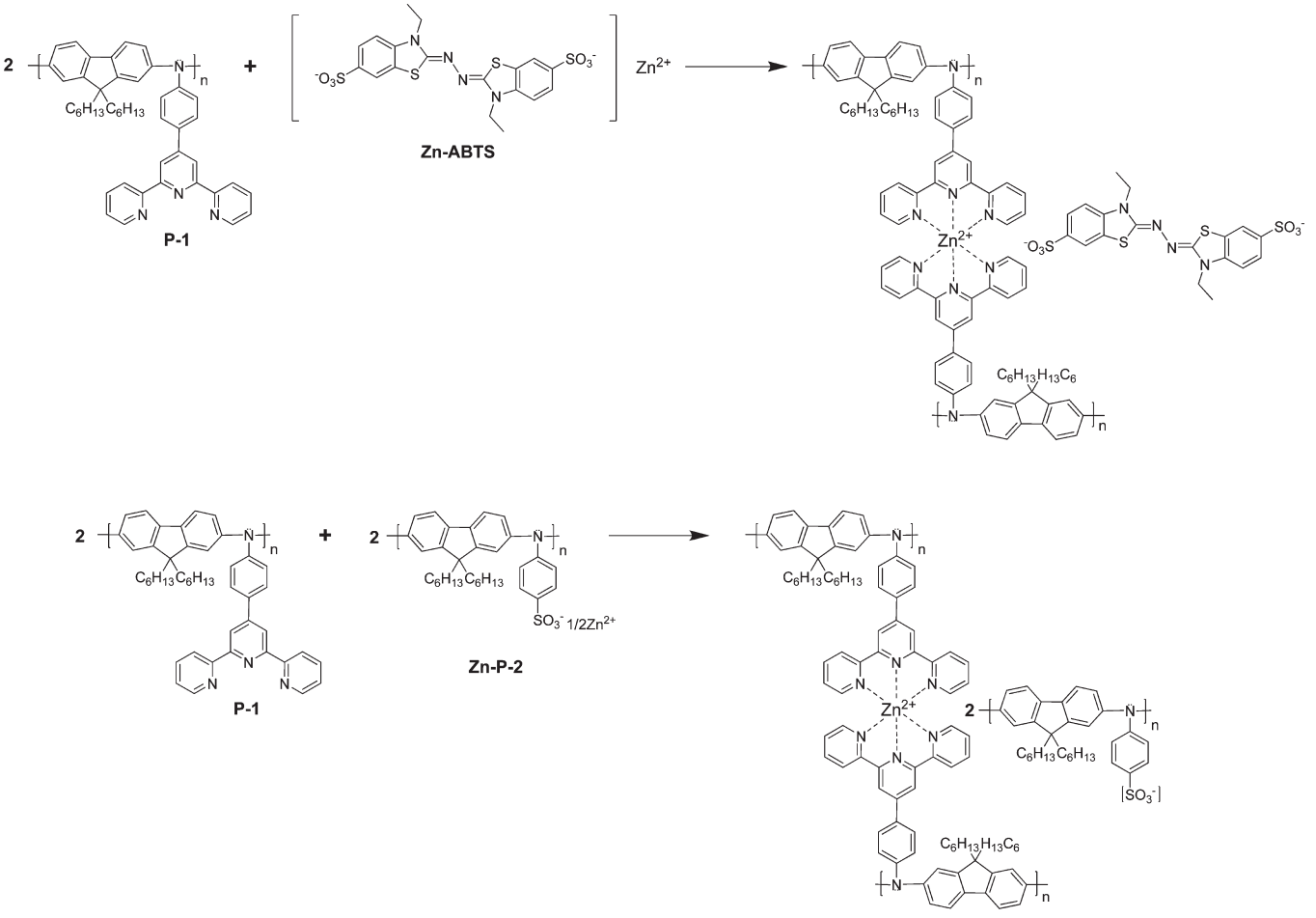

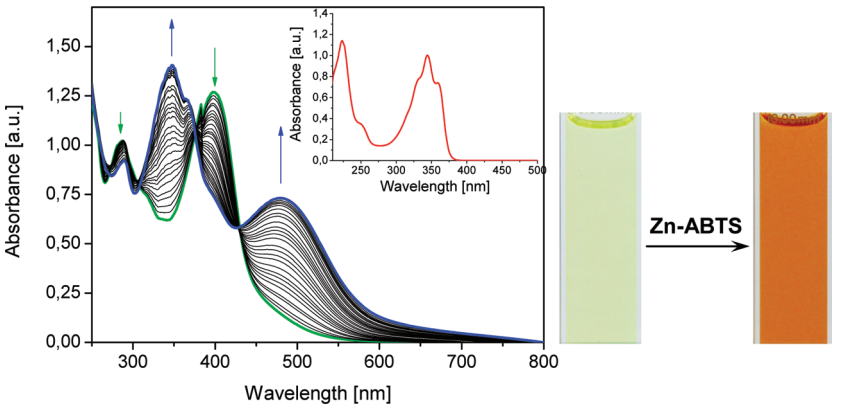

Figure 1. UV/vis absorption spectra of **P-1** (concentration: 1.22×10^{-6} monomol L^{-1}) in THF/methanol (2:1 v/v) prior and subsequent to addition of increasing amounts of **Zn-ABTS** (concentration: 0.93×10^{-5} mol L^{-1}) in the same solvent structure. The inset shows the absorption spectrum of **ABTS** in THF/methanol (2:1 v/v). Photographic images of the polymer solution are also shown.

the complex formation between the two compounds in solution. This study was carried out because one can expect that the UV absorption of the complex formed in solution is similar to the one in the self-assembled films. The complex formation was studied upon titration of a solution of the polymer in THF/methanol (2:1 v/v) with a solution of **Zn-ABTS** in the same solvent mixture. The complexation of the zinc ions with the tpy ligands of the polymer is outlined in Scheme 4a. As indicated in Scheme 4, the **ABTS** dianions represent the counterions neutralizing the positive charge of the zinc-bis-terpyridine complex.

During titration, the absorption bands of the polymer at 286 and 400 nm decrease in intensity, and new bands at 288, 343, and

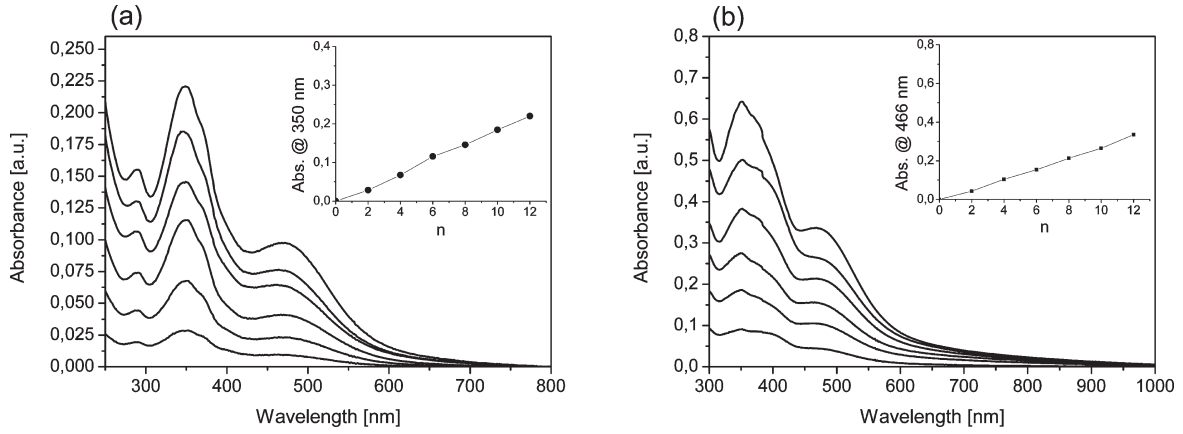

Figure 2. UV/vis absorption spectra of (a) **P-1**/**Zn-ABTS** films and (b) **P-1**/**Zn--2** films monitored after *n* different numbers of dipping cycles. The insets show plots of the absorbance at 350 (a) and 466 nm (b) vs *n*.

480 nm and a shoulder at 365 nm appear. The color of the solution changes from yellow to red orange (see Figure 1). While the 343 nm maximum and the shoulder at 365 nm can be ascribed to the addition of **ABTS** (also see the inset of Figure 1, showing the solution spectrum of the diammonium salt of **ABTS**), the maxima at 288 and 480 nm can be related to the formation of the polymer−Zn ion complex. The end point of the titration was reached, when 0.5 equiv of Zn ions were added, i.e. when the Zn-tpy bis-complex was formed. The occurrence of four clear isosbestic points at 272, 305, 375, and 429 nm indicates a single transition from the noncomplexed to the complexed state.

The color transition is similar to that previously observed[27] for the addition of zinc diacetate to a solution of **P-1**, except that the maximum absorption occurred at 450 nm. The red-shift may be caused by the use of another solvent mixture (THF/methanol 25:1 v/v) and by the fact that the **ABTS** counterion is a dianion with different sterical demand, which may force the polymer backbone into a different conformation, while the complexation with the Zn ions takes place. Although the complex formation proceeds under cross-linking (see Scheme 4a), no gel formation or precipitation was observed. Possible reasons are the low polymer concentration in solution, and the formation of colloidal aggregates of the complex, which are stabilized by the polar solvent mixture.

3.3. Coordinative Sequential Assembly and Optical Properties of Films. *Films Prepared from **P-1** and **Zn-ABTS**.* As the next step, we tried to build up coordination polymer films based on **P-1** and **Zn-ABTS**. The **Zn-ABTS** solution was obtained by adding zinc acetate to a solution of the diammonium salt of **ABTS** in methanol/THF/*n*-hexane (2:1:1 v/v). **P-1** was dissolved in a THF/*n*-hexane (2:1 v/v) mixture. Details of the film formation are described in the Experimental Part. Films were deposited on quartz substrates and analyzed by monitoring the UV/vis absorption after *n* dipping cycles. As shown in Figure 2a, the optical absorption increases linearly with *n*. This indicates a homogeneous deposition (i.e., in each dipping cycle, the same amount of material is deposited). The spectra show three absorption maxima of 290, 350, and 470 nm, which is in good agreement with the maxima obtained upon the complex formation in solution shown in Figure 1. The film exhibits a yellowish orange color. The spectra prove the deposition of the polymer−Zn ion complex with **ABTS** counterions on the substrate. Since the spectra in film and solution are very similar, it is likely that the **ABTS** anions attain a random orientation in the films. There is no indication of aggregate formation.

*Films Prepared from **P-1** and **Zn-P-2**.* The **P-1**/**Zn-P-2** films were prepared in a similar way. The zinc salt of **P-2** was obtained by adding zinc acetate to a solution of **P-2** in methanol. Again, the details of film formation are given in the Experimental Part. The film growth was analyzed using UV/vis spectroscopy. As shown in Figure 2b, the films exhibit absorption bands with maxima at 355 and 466 nm. The intensity increases linearly with the number of dipping cycles *n*, indicating homogeneous film growth. While the broad band with a maximum at 355 nm and a shoulder at 380 nm can be ascribed to the fluorene absorption of the two polymers, the 466-nm absorption probably originates from charge transfer between the electron-donating aminophenyl group of **P-1** and the Zn^{2+}-terpyridine moieties. The complex formation between **P-1** and **Zn-P-2** is outlined in Scheme 4b. The film exhibits a yellow color. From the optical spectra, no conclusions on the structural arrangement of the polymers in the film can be drawn.

3.4. Electrochemical and Electrochromic Properties of Films. For the electrochemical study, the films were deposited on ITO-coated glass supports. Films of the Zn ion complex of **P-1** with **ABTS** and **P-2** counterions were investigated. Twelve dipping cycles were applied.

*Films Prepared from **P-1** and **Zn-ABTS**.* In Figure 3a, the CV diagram of a film with **ABTS** counterions cycled between −750 mV and +750 mV (vs ferrocene/ferrocenium redox couple, FOC) is shown. Two anodic waves appear with peak currents at potentials of 220 and 640 mV (vs FOC). They can be ascribed to the overlapping oxidation of the polymer and the **ABTS** dianions with the formation of the cation radical and dication states. The oxidation is accompanied with a color change of the films from yellow to brownish gray and finally blue. If the potential is decreased again, some overlapping waves with peak currents at +620, 380, and 120 mV occur, which are dominated by the peak at 120 mV. They can be ascribed to reduction of the oxidized polymer and the **ABTS** counterions into the neutral state. The voltammogram indicates a well-reversible oxidation behavior, which essentially represents a superposition of the oxidation of polymer and **ABTS** dianions.

For a more-detailed analysis of the color changes, a spectroelectrochemical study was carried out. Absorption spectra were monitored while different potentials were applied. Spectra and photographs of the films at different potentials are shown in Figure 4a. The film changes color from yellow to brownish gray at

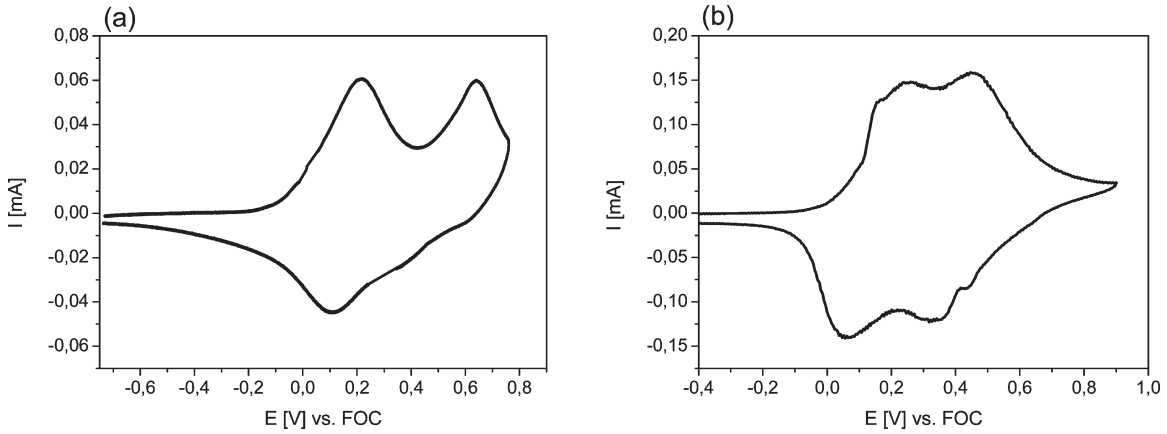

Figure 3. Anodic voltammetric cycles of coordination polymer films of (a) **P-1** and **Zn-ABTS** (12 dipping cycles) and (b) **Zn-P-2** (12 dipping cycles) on ITO-coated glass support.

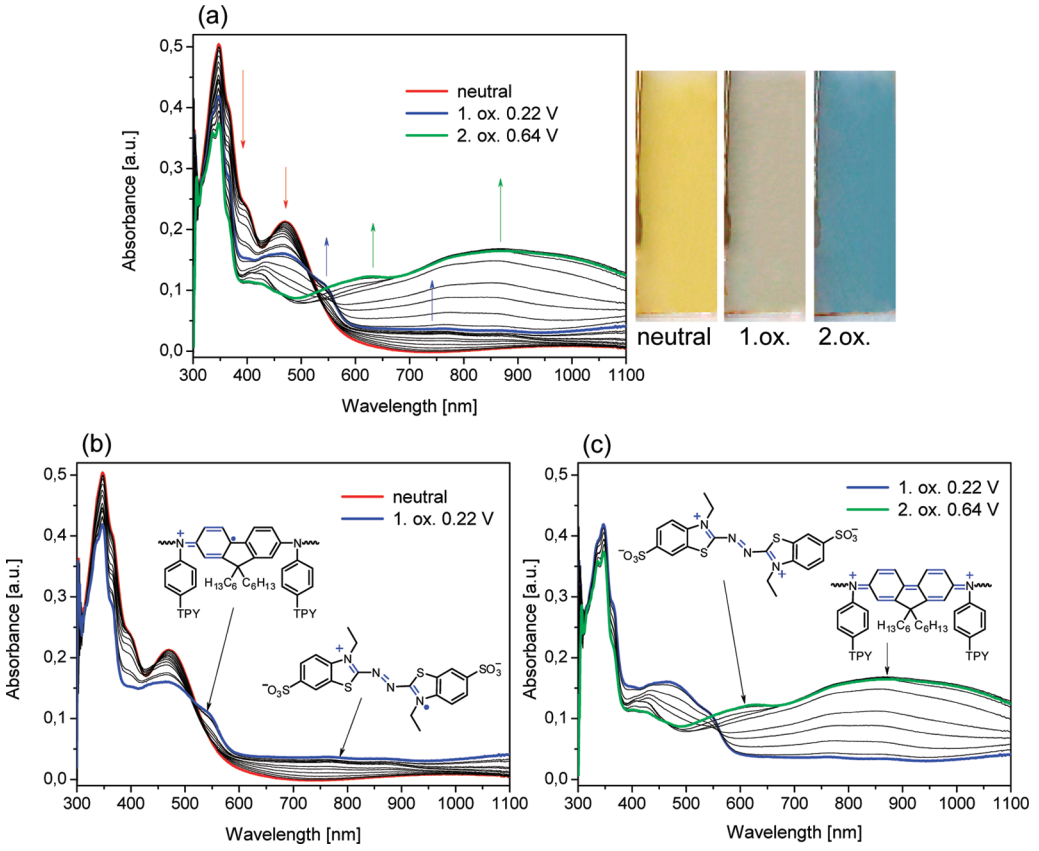

Figure 4. (a) Spectroelectrochemistry of **P-1**/**Zn-ABTS** films (12 dipping cycles) on ITO-coated glass support. Photographs show the colors of the film in the neutral and oxidized states. (b,c) Separate representation of spectral changes during first oxidation of **P-1** and **ABTS** (panel b) and second oxidation of **P-1** and **ABTS** (panel c).

a potential of 220 mV, where the first anodic wave exhibits a maximum. The strong band at 355 nm originates from **ABTS**, and the shoulder at 380 nm and the maximum at 466 nm originate from the polymer. They decrease in intensity, while a new band (shoulder) at 535 nm appears, and the absorption between 500 nm and the infrared region generally increases. While the new absorption band at 535 nm can be ascribed to the oxidation of **P-1**, the oxidation of **ABTS** is responsible for the broad increase of the absorption extending to the infrared (Figure 4b). The color change involves an isosbestic point at ~520 nm. If the potential is further increased to the potential of the second oxidative wave at 640 mV, the film changes its color to blue. The absorption at 355 nm decreases further and the absorption of the polymer at 380 and 466 nm completely disappear. Instead, a new broad band with a maximum at ~800 nm appears, which can be ascribed to the dication state of the polymer, and a weakly pronounced maximum at 620 nm, which can be ascribed to the dication state of **ABTS** (Figure 4c).

dx.doi.org/10.1021/am2004976 |*ACS Appl. Mater. Interfaces* 2011, 3, 2710–2718

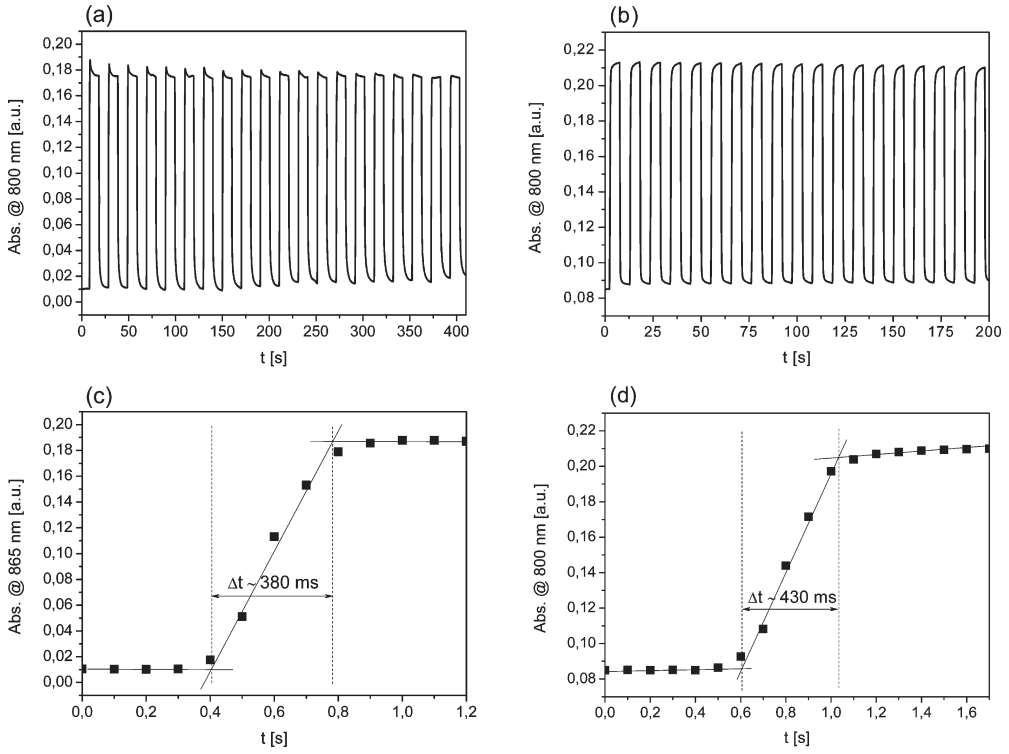

Figure 5. (a,b) Electrochromic switching of coordination polymer films (**P-1**/**Zn-ABTS** (panel a) and **P-1**/**Zn-P-2** (panel b)) on ITO-coated glass supports (12 dipping cycles). The potential was switched between −650 mV and +650 mV (panel a) and −450 and +450 mV (vs FOC) (panel b) every 5 s, and the absorption at 800 nm was monitored versus time. The first 20 cycles are shown (0.1 M $TBAPF_6$/acetonitrile electrolyte/solvent couple). (c,d) Determination of switching time for an **ABTS**-containing film (panel c) and a **P-2**-containing film (panel d). Absorption at 800 nm is plotted versus time after increasing the potential from −650 mV to +650 mV (panel c) and from −450 mV to +450 mV (vs FOC) (panel d) (0.1 M $TBAPF_6$/acetonitrile electrolyte/solvent couple).

Table 1. Characteristic Data of Electrochromic P-1-Based Films

				Contrast, Δ%T		Contrast/Thickness Δ%T [nm]	
	dipping cycles	film thickness [nm]	switching time Δt [s]	at 800 nm	at 630 nm	at 800 nm	at 630 nm
P-1/$Zn(PF_6)_2$	12	46.7	0.450	18		0.380	
		54.0			14.5		0.268
P-1/**Zn-ABTS**	22	88.0	0.380	33	24.7	0.375	0.283
P-1/**Zn**−**P-2**	12	56.0	0.430	27	n.d.[a]	0.480	n.d.[a]

[a] Not determined.

Basically, the spectra represent a superposition of the absorption behavior of the polymer and **ABTS** in their fully oxidized (dication) states. The color changes are highly reversible even if the films are not protected against humidity or oxygen.

The strong color changes from the neutral to the fully oxidized states of **P-1** and **ABTS** were used to determine response time and contrast of the films. For determination of the response time, the potential of 640 mV was switched on and off for time periods of 10 s, and the absorbance at 800 nm was plotted versus the time. The experiments were carried out under ambient conditions. In Figure 5a, the first 20 changes of the absorbance are shown. It can be seen that there is only a slight loss in intensity upon the switching, which indicates a certain stability of the films. Expansion of the time scale allowed for determination of the response time, as shown in Figure 5c. For an 88-nm-thick film prepared from **P-1** and **Zn-ABTS** in 22 dipping cycles, the switching time was 380 ms (see Table 1). The contrast was determined by evaluating the change of the transmission at 800 nm (Δ%T), if a potential of 640 mV was applied. For the film described above, a contrast of 33% was determined (see Table 1). If the absorption at 630 nm is evaluated, the contrast is 24.7%. For a corresponding film of **P-1** and zinc dihexafluorophosphate (12 dipping cycles, with a thickness of 54 nm), the contrast at 630 nm is only 14.5%.[17]

Quite obviously, the introduction of **ABTS** counterions leads to a change in the electrochromic film properties. The reason is that both the polymer−Zn ion complex and the counterion undergo color changes, if an electrical potential is applied. Unfortunately, **ABTS** exhibits a transition from colorless to blue

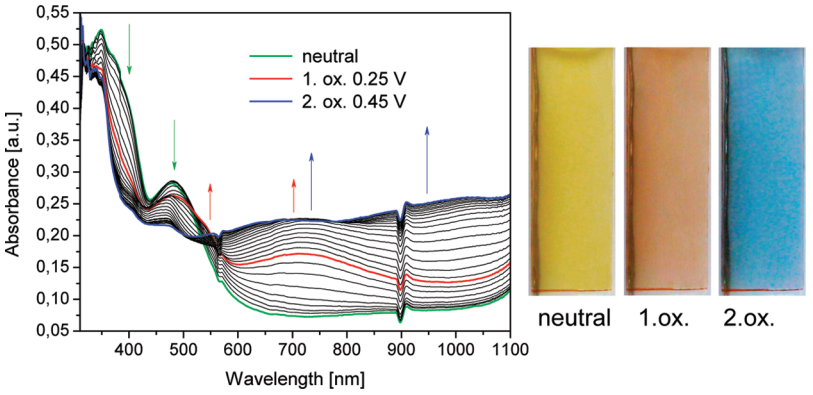

Figure 6. Spectroelectrochemistry of **P-1**/**Zn**−**P-2** film (12 dipping cycles). Photographs show the colors of the film (24 dipping cycles) in the neutral and oxidized states.

and red, while the polymer changes color from yellow to red and blue, and the combination of both does not result in a strong enhancement of the contrast. However, the response time became shorter, probably because the presence of the bulky **ABTS** dianions leads to a larger free volume in the films, which renders an ion transport during switching easier.

*Films Prepared from **P-1** and **Zn-P-2***. It was hoped that the incorporation of counterions containing the same polymer backbone as **P-1** might lead to increased absorbance and higher contrast of the films. The CV diagram of a film prepared from **P-1** and the zinc salt of **P-2** (12 dipping cycles) is shown in Figure 3b. Because of the same backbone in both polymers, the oxidation behavior is similar and only two reversible steps occur: the formation of the cation radical and the dication state, as previously discussed (see Scheme 3). The anodic peak potentials occur at +250 mV and 450 mV, while a subsequent reduction takes place at 320 and 60 mV. During oxidation, the color of the films changes from yellow to dark red and finally blue. The CV study also indicates that the oligomeric nature of **P-2** has no decisive influence on its redox behavior.

A spectroelectrochemical study (Figure 6) shows that the color change from yellow to dark red at 250 mV originates from a decrease of the absorption of the two polymers at $\lambda < 510$ nm and an increase at longer wavelengths. At 530 nm, a shoulder occurs, which can be ascribed to the first oxidized state (cation radical state) of **P-1**. Furthermore, the new band with a maximum at 730 nm originates from the cation radical state of **P-2**. The broad band and the maximum at long wavelengths indicate that the electron delocalization of **P-2** is stronger than that for the polytopic ligand **P-1**. The second color change from dark red to blue at 450 mV originates from the almost-complete disappearance of the absorption maxima at wavelengths shorter than 500 nm and the formation of a very broad absorption extending from 500 nm to the infrared with a broad maximum at ~1020 nm. The maximum can be ascribed to the second oxidized state (dication state) of either polymers. The two-step oxidation is also indicated by the occurrence of an isosbestic point at 513 nm in the first oxidation step, and an isosbestic point at 498 nm in the second step.

The experimental procedures for the determination of response time and contrast were the same as those for the **P-1**/**Zn-ABTS** films described above. In Figure 5b, the repeated change in absorbance at 800 nm upon switching between the neutral (yellow) and fully oxidized (blue) state at 450 mV for time periods of 5 s is shown. Although the film was not protected against oxygen and humidity, there is very little change in intensity, indicating that the film is rather stable in the neutral and oxidized state under ambient conditions. The response time was determined as shown in Figure 5d. For a 56-nm-thick film prepared on 12 dipping cycles, a switching time of 430 ms was found. This is slightly shorter than that for films with hexafluorophosphate counterions (see Table 1).[17] For the same film, we also determined the contrast. The change in transmittance at 800 nm (Δ%T) is 27%, which is round about a quarter higher than that for the corresponding film with nonelectrochromic hexafluorophosphate counterions.[17]

4. CONCLUSIONS

The films described in our study are the first example of electrochromic films with two functional compounds prepared upon coordinative assembly. While the electrochromic tpy-substituted polyiminofluorene is bound via coordinative interactions forming a zinc-bis-tpy complex, the electrochromic anions are bound via electrostatic interactions neutralizing the positively charged, tpy-complexed zinc ions. The two functional compounds are oxidized independently from each other, showing color transitions from colorless in the neutral state to blue (or red) in the fully oxidized state. The color changes are reversible under ambient conditions. While previous studies[16,17,19] showed that the variation of the metal ions[17] and the aromatic units[19] in the polytopic ligands allow one to tailor the electrochromic properties of the films, we now demonstrate that the variation of the metal counterion may also alter and improve the electrochromic properties. Furthermore, it is demonstrated that the presence of the same chromophore in a polytopic ligand and counterion enables one to increase the contrast and shorten the response time. Further structural studies are necessary to analyze the mutual arrangement of the polymers and counterions in the film.

■ ASSOCIATED CONTENT

Supporting Information. ^{1}H NMR spectrum of **P-2** is shown. This material is available free of charge via the Internet at http://pubs.acs.org.

■ AUTHOR INFORMATION

Corresponding Author
*E-mail: tieke@uni-koeln.de.

■ ACKNOWLEDGMENT

The Deutsche Forschungsgemeinschaft is thanked for their financial support (Project No. TI219/11-2).

■ REFERENCES

(1) Deb, S. K. *Appl. Opt., Suppl.* **1969**, *3*, 192.

(2) (a) Monk, P. M. S.; Mortimer, R. J.; Rosseinsky, D. R.; *Electrochromism and Electrochromic Devices*; Cambridge University Press: Cambridge, U.K., 2007. (b) Mortimer, R. J. *Chem. Soc. Rev.* **1997**, *26*, 147. (c) Rosseinsky, D. R.; Mortimer, R. J. *Adv. Mater.* **2001**, *13*, 783.

(3) Dyer, A. L.; Grenier, C. R. G.; Reynolds, J. R. *Adv. Funct. Mater.* **2007**, *17*, 1480.

(4) Heuer, H. W.; Wehrmann, R.; Kirchmeyer, S. *Adv. Funct. Mater.* **2002**, *12*, 89.

(5) (a) Bach, U.; Corr, D.; Lupo, D.; Pichot, F.; Ryan, M. *Adv. Mater.* **2002**, *14*, 845. (b) Beaupré, S.; Dumas, J.; Leclerc, M. *Chem. Mater.* **2006**, *18*, 4011. (c) Schwendemann, I.; Hwang, J.; Welsh, D. M.; Tanner, D. B.; Reynolds, J. R. *Adv. Mater.* **2001**, *13*, 634.

(6) (a) Granqvist, C. G. *Sol. Energy Mater. Sol. Cells* **2000**, *60*, 201. (b) Granqvist, C. G. *Phys. Thin Films* **1993**, *17*, 301. (c) Habib, M. A. *Electrochem. Transition* **1992**, 51. (d) de Tacconi, N. R.; Rajeshwar, K.; Lezna, R. O. *Chem. Mater.* **2003**, *15*, 3046. (e) Dautremont-Smith, W. C. *Displays* **1982**, *3*, 67.

(7) (a) Beaujuge, P. M.; Reynolds, J. R. *Chem. Rev.* **2010**, *110*, 268. (b) Mortimer, R. J.; Dyer, A. L.; Reynolds, J. R. *Displays* **2006**, *27*, 2. (c) Huang, S.-W.; Ho, K.-C. *Sol. Energy Mater. Sol. Cells* **2006**, *90*, 491. (d) Li, M.; Patra, A.; Sheynin, Y.; Bendikov, M. *Adv. Mater.* **2009**, *21*, 1707. (e) Durmas, A.; Gunbas, G. E.; Toppare, L. *Chem. Mater.* **2007**, *19*, 6247. (f) Gunbas, G. E.; Durmas, A.; Toppare, L. *Adv. Mater.* **2008**, *20*, 691.

(8) (a) Monk, P. M. S. *The Viologens*; John Wiley & Sons, Ltd.: West Sussex, U.K., 1998. (b) DeLongchamp, D. M.; Kastantin, M.; Hammond, P. T. *Chem. Mater.* **2003**, *15*, 1575.

(9) (a) Chang, C.-W.; Chung, C.-H.; Liou, G.-S. *Macromolecules* **2008**, *41*, 8441. (b) Liou, G.-S.; Chang, C.-W. *Macromolecules* **2008**, *41*, 1667.

(10) (a) Decher, G. *Science* **1997**, *277*, 1232. (b) Decher, G.; Hong, J. D. *Makromol. Chem., Macromol. Symp.* **1991**, *46*, 321. (c) Decher, G.; Lvov, Y.; Schmitt, J. *Thin Solid Films* **1994**, *244*, 772.

(11) (a) Stockton, W.; Rubner, M. *Macromolecules* **1997**, *30*, 2717. (b) Benjamin, I.; Hong, H.; Avny, Y.; Davidov, D.; Neumann, R. *J. Mater. Chem.* **1998**, *8*, 919. (c) Bai, S.; Wang, Z.; Zhang, X.; Wang, B. *Langmuir* **2004**, *20*, 11828. (d) Erel-Unal, I.; Sukishvili, S. A. *Macromolecules* **2008**, *41*, 3962.

(12) (a) Cao, G.; Hong, H.-G.; Mallouk, T. E. *Acc. Chem. Res.* **1992**, *25*, 420. (b) Evens, S. D.; Ulman, A.; Goppert-Berarducci, K. E.; Gerenser, L. J. *J. Am. Chem. Soc.* **1991**, *113*, 5866.

(13) DeLongchamp, D. M.; Hammond, P. T. *Chem. Mater.* **2004**, *16*, 4799.

(14) (a) DeLongchamp, D. M.; Hammond, P. T. *Adv. Mater.* **2001**, *13*, 1455. (b) Cutler, C. A.; Bouguetaya, M.; Reynolds, J. R. *Adv. Mater.* **2002**, *14*, 684.

(15) (a) Schlenoff, J. B.; Laurent, D.; Ly, H.; Stepp, J. *Adv. Mater.* **1998**, *10*, 347. (b) Kim, H.; Pyo, M. *J. Appl. Electrochem.* **2000**, *30*, 49.

(16) Choi, K.; Yoo, S. J.; Sung, Y.-E.; Zentel, R. *Chem. Mater.* **2006**, *18*, 5823.

(17) DeLongchamp, D. M.; Hammond, P. T. *Adv. Funct. Mater.* **2004**, *14*, 224.

(18) Maier, A.; Rabindranath, A. R.; Tieke, B. *Adv. Mater.* **2009**, *21*, 959.

(19) Maier, A.; Rabindranath, A. R.; Tieke, B. *Chem. Mater.* **2009**, *21*, 3668.

(20) Maier, A.; Fakhrnabavi, H.; Rabindranath, A. R.; Tieke, B. *J. Mater. Chem.* **2011**, *21*, 5795.

(21) Constable, E. C.; Thompson, A. M. W. *J. Chem. Soc., Dalton Trans.* **1992**, 3467.

(22) (a) Wild, A.; Schlütter, F.; Pavlov, G. M.; Friebe, C.; Festag, G.; Winter, A.; Hager, M. D.; Cimrová, V.; Schubert, U. S. *Macromol. Rapid Commun.* **2010**, *31*, 868. (b) Hoogenboom, R.; Wouters, M. E. L.; Schubert, U. S. *J. Am. Chem. Soc.* **2005**, *127*, 2913. (c) Schmatloch, S.; van den Berg, A. M. J.; Hofmeier, H.; Schubert, U. S. *Des. Monomers Polym.* **2004**, *7*, 191. (d) Schmatloch, S.; van den Berg, A. M. J.; Alexeev, A. S.; Hofmeier, H.; Schubert, U. S. *Macromolecules* **2003**, *36*, 9943. (e) Schwarz, G.; Bodenthin, Y.; Geue, T.; Koetz, J.; Kurth, D. G. *Macromolecules* **2010**, *43*, 494. (f) Han, F. S.; Higuchi, M.; Kurth, D. G. *Adv. Mater.* **2007**, *19*, 3928. (g) Krass, H.; Papastravou, G.; Kurth, D. G. *Chem. Mater.* **2003**, *15*, 196.

(23) (a) Potts, K. T.; Usifer, D. A. *Macromolecules* **1988**, *21*, 1985. (b) Hanabusa, K.; Nakano, K.; Koyama, T.; Shirai, H.; Hojo, N.; Kuroseb, A. *Makromol. Chem.* **1990**, *191*, 391. (c) Chujo, Y.; Sada, K.; Saegusa, T. *Macromolecules* **1993**, *26*, 6320. (d) Andreopoulou, A. K.; Kallitsis, J. K. *Eur. J. Org. Chem.* **2005**, 4448. (e) Chujo, Y.; Sada, K.; Saegusa, T. *Macromolecules* **1993**, *26*, 6315. (f) Kimura, M.; Horai, T.; Hanabusa, K.; Shirai, H. *Adv. Mater.* **1998**, *10*, 459. (g) Zhang, Y.; Murphy, C. B.; Jones, W. E. *Macromolecules* **2002**, *35*, 630. (h) Aamer, K. A.; Tew, G. N. *Macromolecules* **2007**, *40*, 2737.

(24) (a) Fei, J.; Song, H.-K.; Palmore, G. T. R. *Chem. Mater.* **2007**, *19*, 1565. (b) Song, H.-K.; Palmore, G. T. R. *Adv. Mater.* **2006**, *18*, 1764. (c) Song, H.-K.; Lee, E. J.; Oh, S. M. *Chem. Mater.* **2005**, *17*, 2232.

(25) Therias, S.; Mousty, C.; Forano, C.; Besse, J. P. *Langmuir* **1996**, *12*, 4914.

(26) Scot, S. L.; Chen, W.-J.; Bakac, A.; Espenson, J. H. *J. Phys. Chem.* **1993**, *97*, 6710.

(27) Rabindranath, A. R.; Maier, A.; Schäfer, M.; Tieke, B. *Macromol. Chem. Phys.* **2009**, *210*, 659.

(28) Lee, J. K.; Klaerner, G.; Miller, R. D. *Chem. Mater.* **1997**, *11*, 11083.

(29) Pyrasch, M.; Amirbeyki, D.; Tieke, B. *Adv. Mater.* **2001**, *13*, 1188.

(30) (a) Kanbara, T.; Houma, A.; Hasegawa, K. *Chem. Lett.* **1996**, 1135. (b) Kanbara, T.; Oshima, M.; Imayasu, T.; Hasegawa, K. *Macromolecules* **1998**, *31*, 8725.